ELECTROCATALYSIS OF A MAJOR POLLUTANT, CO_2, TRANSFORMATION INTO USEFUL ORGANIC MATTER – FUNDAMENTAL AND APPLIED CONTRIBUTIONS

MARIA JITARU, ANA-MARIA TOMA, OLTEAN GABRIEL

Faculty of Chemistry & Chemical Engineering, Babes-Bolyai University,
Associated Francophon Laboratory 11, Arany Janos street, 400028 Cluj-Napoca, Romania,
mjitaru@chem.ubbcluj.ro

Abstract. Metal nanorod arrays and nanotubes are expected to exhibit unusual and interesting properties for possible application in electrocatalysis and fuel cell. This work is divided into four main parts:

- Elaboration of the template nanostructure metals (Cu and Cu-Ni)
- Structural characterization (SEM, SEM-EDX) depending on experimental parameters
- Electrochemical characterization of the deposits towards test reaction (oxygen reduction)
- Preliminary data on the electroreduction of CO_2 on these metal nanorods

On Cu nanorods in bicarbonate solution the main reduction product of carbon dioxide is formic acid;on $(Cu\text{-}Ni)_{nano}$ more hydrogen and traces of methane have been obtained.

Keywords: nanocrystalline metals, template electrodeposition, electrocatalytic activity.

1. Introduction

There is significant interest and ongoing research in the preparation and application of nanometer sized materials. The physical and chemical properties of these materials are quite different from those of the bulk phase due to the high surface area to volume ratio [1].

A.M. Bahadir and G. Duca (eds.), *The Role of Ecological Chemistry in Pollution Research and Sustainable Development*,

Nanostructures shaped like long sticks or dowels with a diameter in the nanoscale but having a length that is much longer, from 1 to 200 nm. They may be synthesized on metals or semiconducting materials [1].

Metal nanoparticles are of interest due to their special properties in many aspects, such as catalysis [2–4], template for assembly of nano-sized materials [5], etc. Their properties and applications are strongly dependent on their shapes [6, 7]. Of all the methodologies developed for the production of metal nanoparticles, on either a physical or chemical basis, the electrochemical method [8–10] offers a simple alternative means for high yield production of nanoparticles.

Copper tubes having diameters between about 100 and about 200 nm have been fabricated by electrodeposition of copper into the pores of alumina nanopore membrane. Copper nanotubes are under consideration as alternatives to copper nanorods and nanowires for applications involving thermal and/or electrical contacts, wherein the greater specific areas of nanotubes could afford lower effective thermal and/or electrical resistivities.

The oxygen reduction reaction is very important in many processes, such as electrochemical energy conversion/storage, metal corrosion, fuel cell and electrocatalysis [11–14]. Different materials have been proposed as electrocatalysts for oxygen reduction and the mechanism of electrochemical reduction of molecular oxygen at such electrode materials has been extensively studied [12–14]. The kinetics of oxygen reduction is very important and it could be a measure for the electrocatalytic activity of different electrodes.

In this work we present the preparation and characterization of copper and Cu-Ni nanostructure onto a copper coin by deposition through an alumina membrane that is later dissolved.

The electrochemical reduction of carbon dioxide on metallic electrodes, has been a topic of great interest due to the build up of CO_2 in the atmosphere caused by oxidation of carbon compounds. On the other hand, CO_2 represents a possible potential source for carbon in the manufacturing of chemicals.

2. Experimental section

2.1. Reagents and solution preparation

Copper foil about 0.1mm thickness (Merck, Germany) was used in the process of electrodeposition of the copper nanorods. $CuSO_4 \cdot 5H_2O$ with purity greater than 99% (Remed Prodimpex SRL, Romania), $(NH_4)_2SO_4$ with purity greater than 99% (Aldrich, Germany), diethylene-tri-amine with purity greater than 97% (Fluka, Switzerland), $NaH_2PO_4 \cdot H_2O$ (monobasic) with purity greater than 99% (Fluka, Switzerland), $Na_2HPO_4 \cdot 2H_2O$ (dibasic) with purity greater than 99% (Fluka, Switzerland), NaOH with purity greater than 98% (Lachema, Czech Republic) were used

to prepare the solutions with desirable concentration for the experiments in this study. Distilled water was used to prepare the aqueous solutions. All the treated substances were used without further purification.

2.2. Methods

Voltametric measurements were made using a potentiostat-galvanostat system – AUTOLAB PG-STAT12, Eco Chemie, Netherlands, with the specific software GPES 4.9 and a classic three electrode electrochemical cell. The experimental design consist of a platinum plate auxiliary electrode, an Ag/AgCl, KCl reference electrode, and the working electrodes were copper foil and Cu_{nano} with 2.075 cm^2 active surface.

Nanostructured copper particles were deposited electrochemically on copper foil through an alumina membrane using a deaerated solution of 100g L^{-1} $CuSO_4$ and a phosphate buffer solution (PBS), pH 7, under different applied potentials. Better electrocatalytic activity could be achieved when Cu_{nano} was electrodeposited at 0.4 V at a charge of 50 C. Prior to each experiment, the electrodes were rinsed with deionizer water and sonicated in a water bath for 15 min in ethyl alcohol.

The electrolysis cell consisted of a large (4.15 cm^2) and thin (150 μm) cathode copper current collector foil together with a thick copper anode (500 μm) surrounded by 60 μm thick Anodized Alumina Oxide (AAO) membrane, a porous cellulose separator has been placed in order to avoid the short circuit of the cell. A constant pressure was applied to the stack by means of two stainless steel clamps. The electrolyte bath was consisting of $CuSO_4 \cdot 5H_2O$ 100 gL^{-1}, $(NH_4)_2SO_4$ 20 gL^{-1} and diethyl-tri-amine (DETA) 80 mL L^{-1}. Electrolysis was carried out under pulsed cathodic current, representing a repeated sequence of 300 ms comporting two steps. Initially, a low current density of 2–4 $mA \cdot cm^{-2}$ is applied to the copper cathode for 200 ms followed by a 30 $mA \cdot cm^{-2}$ current density for 50 ms (type A Cu_{nano} electrode) or a low current density of 5 $mA \cdot cm^{-2}$ for 150 ms followed by a 30 $mA \cdot cm^{-2}$ current density for 50 ms (type B Cu_{nano} electrode). The same procedure has been applied for a mixture of 1:1 ($CuSO_4 \cdot 5H_2O$ 50 gL^{-1} and $NiSO_4 \cdot 7H_2O$ 50 gL^{-1}).

The time of electrolysis was 50 min for the type A electrode and 55 min for the type B electrode after which the alumina membrane was dissolved in 1M NaOH for 2 min at 80°C. Finally, the copper foil was washed with distilled water and dried at room temperature.

The electrodeposited $Metal_{nano}$ was characterized by SEM (Scanning Electron Microscopy, JEOL JEM 5510LV) and the composition has been determined by EDX.

The electrocatalytic activity of nanostructured copper particles (represented as type A and type B Cu_{nano}) has been assessed in comparison to the classical Cu electrode, in sodium buffer phosphate solution, pH 7.

3. Results and discussion

3.1. Cu_{nano} electrode structure

Typical SEM morphologies of the products are shown in Fig. 3.1.1. It can be seen that the products mainly consist of rod-like structures.

Figure 3.1.1 shows nanorods obtained under a controlled current of 2 mA cm^{-2} (type A electrode) and 5 $mA \cdot cm^{-2}$ (type B electrode). The mean transverse diameter of a Cu nanorod is about 30 nm, while the mean longitudinal length varies from 400 to 1nm. A higher yield of nanorods was obtained at a current density of 5 $mA \cdot cm^{-2}$. The shape of the nanorods obtained at this current density are different from those obtained at a current density of 2 $mA \cdot cm^{-2}$. There is evidence that the current applied during electrodeposition is of great importance for the structure of Cu_{nano}.

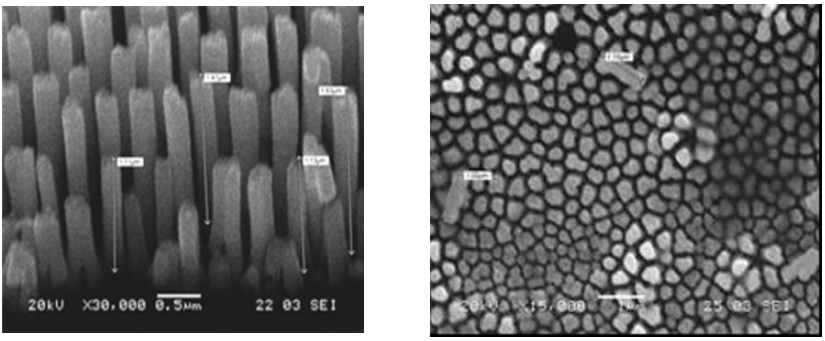

Fig. 3.1.1. SEMs for Cu_{nano} (Scanning microscope JEOL JEM 5510LV).

3.2. $(Cu\text{-}Ni)_{nano}$ electrode structure

From the mixture of Cu-Ni electrolytes, both the homogeneity, structure and stability of Cu-Ni nanorods is affected, Fig. 3.2.1 (a–c); in some experiments, Ni dendrites were obtained on initial copper nanorods, Fig. 3.2.1 (d).

This fact can be explained by the difference between the kinetic characteristics of fast copper and slower nickel electrodeposition.

The morphology of nanorods can be explained according to the one of accepted growing mechanism [15], of primary nucleation of Cu on the surface of AAO membrane and subsequant qrowing of $(Cu\text{-}Ni)_{nano}$ along the pore wall. Figure 3.2.2 shows the SEM images of $(Cu\text{-}Ni)_{nano}$ electrodeposited by method A, from electroytes containing a mixture of 1:1 ($CuSO_4 \cdot 5H_2O$ 50 gL^{-1} and $NiSO_4 \cdot 7H_2O$ 50 gL^{-1}).

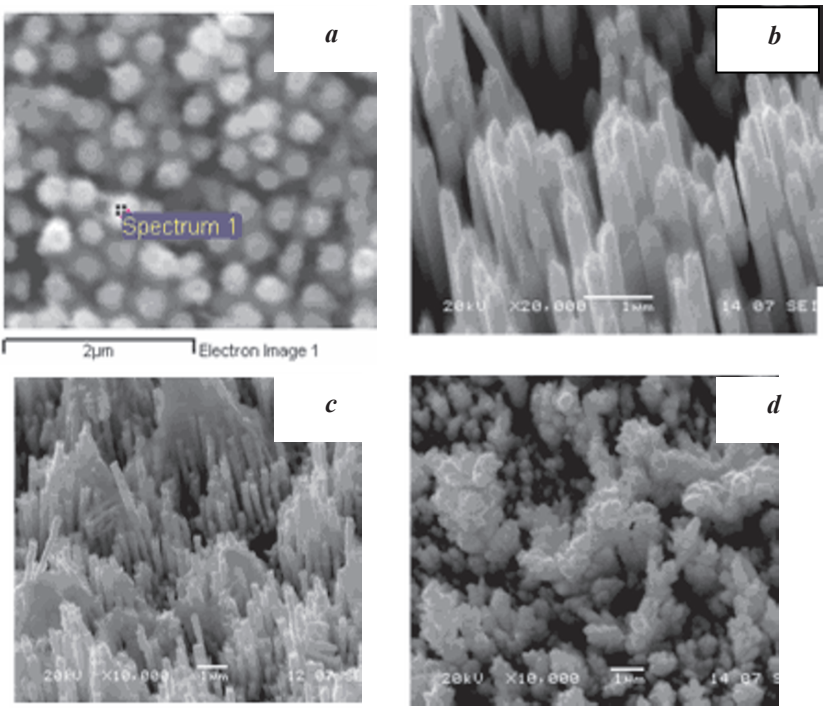

Fig. 3.2.1. SEMs for $(Cu\text{-}Ni)_{nano}$ (a–c) and dendrites formation (d).

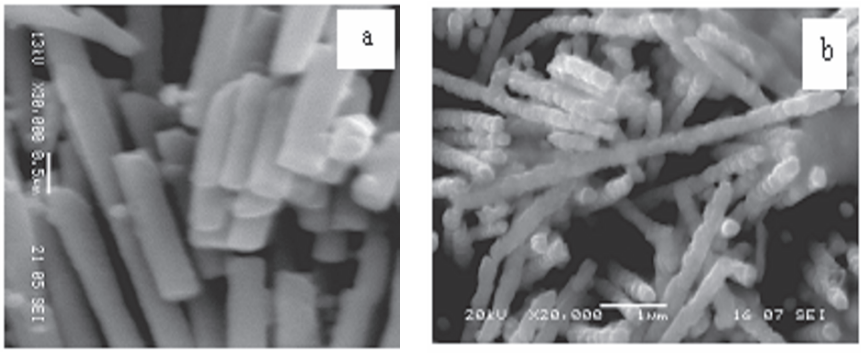

Fig. 3.2.2. SEMs for $(Cu\text{-}B)_{nano}$ (a) and $(Cu_{6.3}\,Ni_1)_{nano}$ (b).

The nanorods arrays have the length of 1.0–1.6 µm and the diameter of 217–290 nm, depending on the experimental parameters. The measured diameter of nanorods is controlled by pore diameter in AAO membrane.

The quantitative EDX analysis of $(Ni\text{-}Cu)_{nano}$ gives information about the composition of final nanostructures, Table 3.2.1. Starting from 1:1 copper and nickel ions in the electrolyte, different Cu-Ni composition from $Cu_{5.28}\,Ni_1$ to $Cu_{11.09}\,Ni_1$ are obtained.

According to these experiments, it is not possible to perform the advanced post treatment of $(Cu\text{-}Ni)_{nano}$ (AAO dissolving and washing) without affecting the nanorods structure. The remaining aluminum 0–6.3%, oxygen 1–19% and carbon 0–15.7%, proceeded, respectively, from AAO membrane and organic surfactant (DETA) in electrolyte. On the other hand, (DETA) is important to stabilize the nanorods.

Table 3.2.1. Quantitative EDX analysis of $(Cu\text{-}Ni)_{nano}$.

Sample	% (weight)					Discussion
	Cu	Ni	Al	O	C	
Cu-A	95.5	–	–	1.1	3.3	–
Cu-B	100	–	–	–	–	See Fig. 3.2.2a: pure $Cu_{nanorods}$ well washed, but pushed of the Cu coin
$(Ni\text{-}Cu)_1$	72.5	11.8	5.7	9.9	–	$Cu_{6.14}Ni_1$
$(Ni\text{-}Cu)_2$	75.2	14.3			10.5	$Cu_{5.28}\,Ni_1$
$(Ni\text{-}Cu)_3$	78.5	7.3	4.7	9.5	–	$Cu_{10.75}\,Ni_1$
$(Ni\text{-}Cu)_4$	58.8	5.3	6.3	19.2	10.4	$Cu_{11.09}\,Ni_1$
$(Ni\text{-}Cu)_5$	72.8	11.4	1.0	3.3	11.5	See Fig. 3.2.2b:$Cu_{6.3}\,Ni_1$ containing high quantities of unwashed (DETA)
Ni	–	80.2	1.0	3.1	15.7	High level of unwashed (DETA)

In this study, some nanostructures were used for oxygen and carbon dioxide electro reduction.

3.3. Electrocatalytic activity of Cu_{nano} for oxygen reduction

The O_2 reduction peak current in PBS at pH 7 is taken as the measure of $Metal_{nano}$ electrochemical reactivity. In the presence of dissolved oxygen in PBS a reduction peak was observed in the cyclic voltammogram as shown in Fig. 3.3.1, comparing to the electrochemical answer on Cu foil.

The dissolved oxygen reduction peak was observed at –1.2 V/Ag,AgCl V at Cu electrode. At type B Cu_{nano} structured electrode oxygen reduction occurs at -0.82 V with a strong decrease in over potential (ΔE = 380 mV) when compared to Cu foil electrode whereas at type A Cu_{nano} structures the results suggests that the electroreduction of oxygen takes place at about –0.65 V. Cu_{nano} electrode can be used for catalytic oxygen reduction in neutral solution. This shift of potential is more important for Cu_{nano} obtained according to (B) procedure, the one obtained at a low current density of 5 $mA{\cdot}cm^{-2}$ for 150 ms followed by a 30 $mA{\cdot}cm^{-2}$ current density for 50 ms.

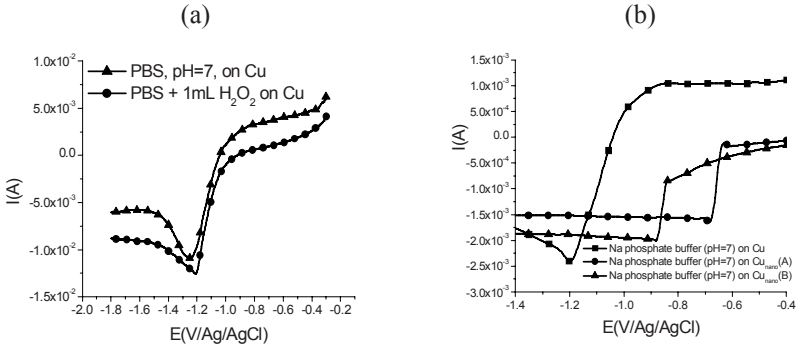

Fig. 3.3.1. Cyclic voltammograms recorded for oxygen reduction at Cu (a) and Cu_{nano} (b) electrodes in PBS in the presence of dissolved oxygen and of oxygenated water.

In the presence of important quantities of H_2O_2 the reduction potential of the oxygen is displaced to 0.9 V. This value is close to the reduction potential of oxygen saturated PBS.

Different forms of Cu_{nano} were deposited on Cu foil at different applied potentials (E_{app}) by electro-deposition and used for oxygen reduction. Figure 3.3.2(a) shows the effect of applied potentials on the oxygen reduction peak currents. The oxygen reduction peak current increased at more negative potentials and reached a maximum at –0.4 V (Fig. 3.3.2 (a)). The difference in the electrochemical behavior of the Cu_{nano} electrode is due to the partially charged copper nanorods (Cu^0 and Cu^+) monolayer formed around 0 to –0.2 V. The partially charged copper nanostructures attributes in some cases to the poor performance for oxygen reduction at Cu_{nano} electrode.

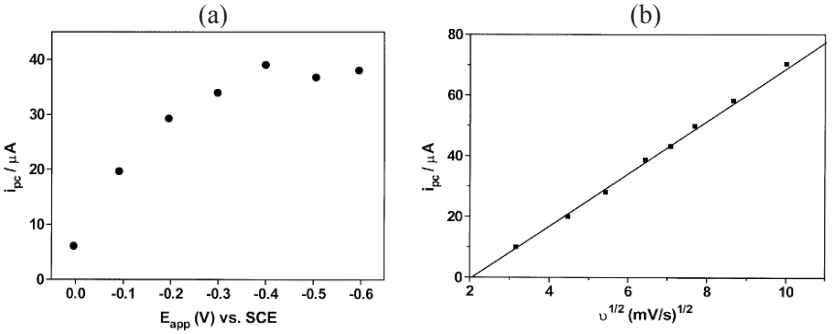

Fig. 3.3.2. Effect of different applied potentials on the formation of Cu_{nano} particles onto alumina/Cu electrode (a); plot of electrocatalytic oxygen reduction peak current (*i*pc) as a function of square root of scan rate observed for oxygen reduction at Cu_{nano} electrode in the presence of oxygen- dissolved in 0.1 M PBS (b).

The linear plot indicates that the oxygen reduction at Cu_{nano} electrode follows diffusion-controlled process, Fig. 3.3.2 (b). This means that the Faradaic current (*ip*) whose magnitude is controlled by the rate at which a reactant in an electrochemical process diffuses toward an electrode/solution interface (and, sometimes, by the rate at which a product diffuses away from that interface) is controlled by diffusion of the analytes.

$(Cu\text{-}Ni)_{nano}$ is also a high-active oxygen reduction electrocatalyst, having the oxygen reduction potential in the same region. But these results were not reproducible so far, probably due to a complex structure of template co-deposited Ni. Further investigations are necessary in order to establish and to confirm the oxygen reduction potential for this structure.

It should be noted that the cathodic peak current observed during oxygen reduction includes the current due to the reduction of metal oxides, if any, to metal (0). It is impossible to separate these two contributions accurately. However, the cathodic limiting currents observed during oxygen reduction at the Cu_{nano} electrodes were much larger than that of the peak currents observed for the cuprous oxide reduction, which was confirmed from the cathodic peak currents observed in the deaerated solution. Thus, it is reasonable to conclude that the major con tribution to the peak current comes from the catalytic oxygen reduction reaction, (Scheme 1).

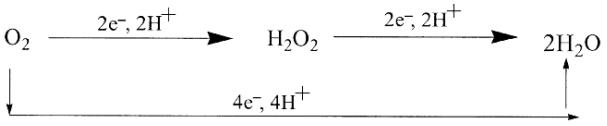

Scheme 3.3.1. Oxygen reduction to H_2O by two pathways.

3.4. Preliminary data on carbon dioxide electroreduction

The Cu_{nano} (A), Cu_{nano} (B) and $(Ni\text{-}Cu)_2$ from the Table 3.2.1 were used for carbon dioxide reduction in aqueous medium (0.2 M K_2CO_3) under CO_2 atmosphere (14–25)°C. The electro-reduction of CO_2 was performed in a laboratory divided bench-scale reactor (V = 200 ml; Nafion 424 membrane), equipped with specified cathodes (S = 2.2 cm^2) and Pt anode. The faradic efficiencies of formation for the main products were calculated from the total charge passed during batch electrolyses, which was set to 50 coulombs.

During the preparative electrolysis, 5 mL electrolyte samples were taken (in 30 min periods) These samples were studied with respect to form formic acid. Gas chromatography [16] and TOC analyses have been applied.

The best results (64% faradic efficiency) was obtained on Cu_{nano} (B) at 14°C; whereas on $(Ni\text{-}Cu)_2$ cathode 59% average faradic efficiency was observed for the formation of formic acid at the same temperature.

4. Conclusions

During these experiments, the most important problem was the reproducibility and homogeneity of the Cu_{nano} and $(Cu\text{-}Ni)_{nano}$ deposits and the oxidation stability of the nanostructures obtained. Accordingly, freshly obtained Me_{nano} electrodes were used for each experiment.

The difference in the electrochemical behavior of the Cu_{nano} and $(Cu\text{-}Ni)_{nano}$ electrode for the electrochemical dissolved oxygen reduction is due to the applied current and the partially charged metal nanostructures (Me^0 and Cu^+), formed around 0 to –0.2 V. The oxygen reduction at Cu_{nano} electrode follows diffusion-controlled process.

The current efficiency for main product formation in solution (formate) depended on the current density and was found to be up to 64% at high negative potential (–1.7 V/SCE) decreasing with operating time and increasing temperature: 59–64% at 14°C and 45–50% at 25°C.

The future objective is to obtain more stable nanostructures in order to obtain data on the electrocatalytic activity over time.

From the ecological point of view, carbon dioxide transformation in useful organic matter will be of great interest in the future. In this connection, the electrochemical reduction of CO_2 using the reported nanostructures and requiring only an additional input of water and electrical energy, appears an attractive possibility to prepare formic acid and hydrocarbons.

Acknowledgments. This work has been supported by Romanian PN II "ELCAT-CO_2" project 32114/2008-2011. The participation to NATO ARW "The Role of Ecological Chemistry in Pollution Research and Sustainable Development" Chisinau, October 8–12, 2008 has been supported by the organizers.

References

1. M.T. Reetz, W. Helbing, S.A. Quaiser, U. Stimming, N. Breuer, R. Vogel, Visualization of surfactants on nanostructured palladium clusters by a combination of STM and high-resolution TEM, *Science,* **1995, 267 (5196),** 367–369.
2. R.L.V. Wal, Flame synthesis of substrate-supported metal-catalyzed carbon nanotubes, *Chemical Physics Letters,* **2000, 324 (1–3),** 217–223.
3. Y. Li, J. Liu, Y. Wang, Z.L. Wang, Preparation of monodispersed Fe-Mo nanoparticles as the catalyst for CVD synthesis of carbon nanotubes, *Chemical Materials,* **2001, 13,** 1008–1014.
4. J.S. Lee, G.H. Gu, H. Kim, W.S. Jeong, J. Bae, J.S. Suh, Growth of carbon nanotubes on anodic aluminum oxide templates: fabrication of a tube-in-tube and linearly joined tube, *Chemical Materials,* **2001, 13 (7),** 2387–2391.
5. B.E. Baker, M.J. Natan, H. Zhu, T.P. Beebe, Au colloid monolayers as templates for nanotructure assembly, *Supermolecular Science,* **1997, 4 (1–2),** 147–154.

6. F. Kim, J.H. Song, P. Yang, Photochemical synthesis of gold nanorods, *Journal of American Chemical Society,* **2002, 124 (48)**, 14316–14317.
7. C.J. Murphy, N.R. Jana, Controlling the aspect ratio of inorganic nanorods and nanowires, *Advanced Materials*, **2002, 14 (1),** 80–82.
8. M.T. Reetz, W. Helbig, Size-selective synthesis of nanostructured transition metal clusters, *Journal of American Chemical Society,* **1994, 116,** 7401–7402.
9. S.Y. Zhao, S.B. Lei, S.H. Chen, H.Y. Ma, S.Y. Wang, Assembly of two-dimensional ordered monolayers of nanoparticles by electrophoretic deposition, *Colloid and Polymer Science,* **2000, 278 (7),** 682–686.
10. S.Y. Zhao, S.H. Chen, S.Y. Wang, S.B. Lei, Z.L. Quan, The gas sensitivity of a metal-insulator-semiconductor field-effect-transistor based on Langmuir–Blodgett films of a new asymmetrically substituted phthalocyanine, *Thin Solid Films,* **2000, 360 (1–2),** 256–260.
11. V.S. Murthi, R.C. Urian, S. Mukerjee, Oxygen reduction kinetics in low and medium temperature acid environment: correlation of water activation and surface properties in supported Pt and Pt alloy electrocatalysts, *The Journal of Physical Chemistry,***2004, B108 (30),** 11011–11023.
12. B. Sljukic, C.E. Banks, R.G. Compton, An overview of the electrochemical reduction of oxygen at carbon-based modified electrodes, *Journal of the Iranian Chemical Society,***2005, 2 (1),** 1–25.
13. I. Yagi, T. Ishida, K. Uosaki, Electrocatalytic reduction of oxygen to water at Au nanoclusters vacuum-evaporated on boron-doped diamond in acidic solution, *Electrochemistry Communications,* **2004, 6(8),** 773–779.
14. V. Soukharev, N. Mano, A. Heller, A four-electron O_2-electroreduction biocatalyst superior to platinum and a biofuel cell operating at 0.88 V, *Journal of American Chemical Society,* **2004, 126 (27),** 8368–8269.
15. S. Xue, C. Cao, H. Zhu, Electrochemically and template synthesized nickel nanorod arrays and nanotubes, *Journal of Materials Science,* **2006, 41,** 5598–5601.
16. T. Kotel'nikova, O. Vdovenko, S. Voronina, A. Perkel, Gas-chroma-tographic determination of formic acid in the oxidation products of organic substances, *Journal of Analytical Chemistry,* **2006, 61(4)**, 338–342.